Method Article

A site-specific standard for comparing dynamic solar ultraviolet protection characteristics of established tree canopies

N.J. Downs[a,*], H.J. Butler[a], L. Baldwin[b], A.V. Parisi[a], A. Amar[c], J. Vanos[d], S. Harrison[c]

[a] Centre for Applied Climate Sciences, University of Southern Queensland, Toowoomba, Australia
[b] Queensland University of Technology, Faculty of Health, Brisbane, Australia
[c] School of Agricultural, Computational and Environmental Sciences, University of Southern Queensland, Toowoomba, Australia
[d] Arizona State University, School of Sustainability, Tempe, AZ, United States

ABSTRACT

A standardised procedure for making fair and comparable assessments of the ultraviolet protection of an established tree canopy that takes into account canopy movement and the changing position of the sun is presented for use by government, planning, and environmental health authorities. The technique utilises video image capture and replaces the need for measurement by ultraviolet radiometers for surveying shade quality characteristics of trees growing in public parks, playgrounds and urban settings. The technique improves upon tree shade assessments that may be based upon single measurements of the ultraviolet irradiance observed from a fixed point of view. The presented technique demonstrates how intelligent shade audits can be conducted without the need for specialist equipment, enabling the calculation of the Shade Protection Index (SPI) and Ultraviolet Protection Factor (UPF) for any discreet time interval and over a full calendar year.

- Tree shade UPF measurements are presented using video capture analysis of moving canopies
- A standard method for making accurate assessments of tree shade has been developed
- Tree shade comparisons are made without the need for specialist equipment

* Corresponding author.
  E-mail addresses: nathan.downs@usq.edu.au (N.J. Downs), harry.butler@usq.edu.au (H.J. Butler), l.baldwin@qut.edu.au (L. Baldwin), parisi@usq.edu.au (A.V. Parisi), Abdurazaq.amar@usq.edu.au (A. Amar), Jenni.vanos@asu.edu (J. Vanos), simone.harrison@usq.edu.au (S. Harrison).

Specifications Table

Subject Area:	Environmental Science
More specific subject area:	Solar radiation measurement
Method name:	Measuring the ultraviolet protection of tree shade from canopy video analysis
Name and reference of original method:	Grant, R., Heisler, G., Gao, W., 2002. Estimation of pedestrian level UV exposure under trees, Photochem. Photobiol., vol. 75, pp. 369-376.
	Downs, N.J., Baldwin, L., Parisi, A.V., Butler, H.J., Vanos, J., Beckman, M., Harrison, S. 2019. Comparing the annualized dynamic shade characteristics of twenty-one tree canopies across twenty-six municipalities in a high ambient UV climate, Queensland – Australia, Appl. Geogr. vol. 108, pp.74-82.
Resource availability:	N/A

Method details

The objective of this method is to provide a standardised assessment procedure for determining the broad-spectrum, and biologically effective ultraviolet shade quality of an established tree growing at any latitude or within a range of environments. This technique was recently applied to assess the solar ultraviolet protection characteristics of 21 individual trees [1]. The developed method is intended to enable government, planning, design, built environment and health authorities to conduct intelligent shade audits without the need for specialised equipment that takes into account the natural movement in a tree canopy and the changing position of the sun throughout the day and calendar year. In this work, the method for measuring the SPI and UPF of a single tree canopy of the species *Araucaria bidwillii* is presented. The derived canopy UPF of *Araucaria bidwillii* is compared against radiometer measurements taken under the same tree on 7 November 2018.

Definition of shade assessment metrics (SPI & UPF)

Tree canopies intercept potentially harmful solar radiation before reaching the Earth's surface (Fig. 1a). This radiation consists of two components, the available direct (or shadow causing) solar radiation, and diffuse radiation scattered by the atmosphere and visible as blue skylight. Dense tree canopies are effective in blocking direct sunlight and produce dark, clearly defined surface shadows. Tree canopies that cover a large surface area provide greater levels of direct shading and are also effective in reducing the diffuse skylight that contributes to the total available solar radiation reaching the surface. The influence of a tree canopy upon this radiation can be measured provided the sky view underneath the canopy and position of the sun is known (Fig. 1b). The solar radiation reaching the surface after passing through a tree canopy may therefore be determined using the approximation of Grant et al. [2]:

$$I_s = (I_{dir} \times P_o) + (I_{diff} \times F_s) \tag{1}$$

where I_s is the total solar irradiance that reaches the surface after passing through a tree canopy. I_{dir} and I_{diff} are the direct and diffuse solar irradiance components at the top of the canopy respectively. P_o is the probability that the direct solar radiation will pass through the tree canopy and F_s is the visible sky fraction observed from underneath the canopy.

The quality of protection provided by any tree is dependent on the available solar UV radiation (290–400 nm) that penetrates the canopy and reaches the surface. The shortest wavelength optical solar radiation able to reach the Earth's surface after atmospheric absorption may be defined as I(UV). I(UV) is biologically effective to humans, where excessive exposure has the potential to cause noticeable short term damage to the skin and eye in addition to several long term diseases and conditions, including keratinocyte and melanoma skin cancer [3,4],

$$I(UV) = \int_{290}^{400} I_{dir}(\lambda) \ d\lambda \ + \int_{290}^{400} I_{diff}(\lambda) \ d\lambda \ . \tag{2}$$

The level of protection from solar radiation that causes harm to humans may be expressed as a fraction of the total available solar UV surface radiation under a tree canopy, $I_s(UV)$ relative to the available ambient, $I(UV)$ at the top of the canopy where $I(UV)$ is the sum of both direct I_{dir}, and diffuse I_{diff}, solar UV components. Here, $I_s(UV)$ is determined by application of Eq. (1) for wavelengths, λ in the solar UV range and is dependent on the probability of direct solar UV penetrating the canopy at a given time of day, and the available sky fraction. For the developed method, the effective protection of a tree canopy from solar radiation that has the potential to cause harm is expressed as the ultraviolet Shade Protection Index (SPI):

$$SPI = \frac{I(UV)}{I_s(UV)} \quad . \tag{3}$$

The SPI is effectively the unweighted Ultraviolet Protection Factor (UPF) and represents the relative protection of a tree canopy from all UV wavelengths in the 290 to 400 nm range that reach the surface of the earth. The UPF is a similar metric, commonly applied to assess the protection of built shade structures, and textiles including beach umbrellas and shade sails. The difference between the SPI and UPF is that the UPF is spectrally weighted to the erythema action spectrum for human skin [5], $A_{ery}(\lambda)$. The UPF may therefore be defined as,

$$UPF = \frac{\int_{290}^{400} I_{dir}(\lambda)A_{ery}(\lambda) \ d\lambda + \int_{290}^{400} I_{diff}(\lambda)A_{ery}(\lambda) \ d\lambda}{\int_{290}^{400} I_s(\lambda)A_{ery}(\lambda) \ d\lambda} \quad . \tag{4}$$

The relative protection provided by a tree canopy from solar ultraviolet radiation will vary according to Rayleigh's criterion for preferential atmospheric scattering of shorter UV wavelengths, which increases with higher air mass and results in a greater proportion of short wavelength diffuse UV being available during the early morning and late afternoon. The UPF is therefore sensitive to changes in the diffuse and direct solar UV irradiance distribution as the human erythema action spectrum, $A_{ery}(\lambda)$ preferentially weights the available solar UV radiation to UVB wavelengths (290 to 315 nm) and has minimal influence in the UVA (315 to 400 nm). Thus, the UPF (Eq. (4)) of a given tree canopy will differ from the SPI (Eq. (3)) due to differing diurnal proportions in the direct and diffuse short wavelength ambient solar radiation available at the top of a tree canopy at any given time of day.

The unweighted SPI and erythematic UPF are both used here as a measure of the environmental UV protection provided by a tree canopy. Utilising the SPI to derive the UV protection of a tree canopy accounts for any potential biological bias introduced by weighting to the human erythema action spectrum. Including the SPI also takes into account the potential carcinogenic influence of the available UVA wavelengths [6] which are more abundant at the Earth's surface [7], and penetrate deeper into human skin tissue [8,9]. The UPF is a standard metric for expressing human biological protection to solar UV radiation [10,11]. However, because the SPI and UPF vary with time of day, season, local latitude (and longitude), standardised assessment procedures are required to objectively compare the quality of protection provided by a tree canopy, including when the sun is blocked (Fig. 2a) and not blocked by the canopy structure (Fig. 2b).

Measuring the dynamic sky view of a tree canopy

Measured sky fraction changes depending on the location of the tree canopy observation point. To make fair assessments that can be used to compare of the quality of tree shade between different tree species (and specimens), the method introduced here (Southern hemisphere) requires all canopy measurements to be made due north of the tree trunk and midway between the trunk and approximate canopy circumference (Fig. 3). For canopy measurements made in the Northern hemisphere, this point would be located due south of a given tree trunk. To find the location of this point for our example tree *Araucaria bidwillii*, the approximate canopy circumference was calculated from the longest and shortest canopy diameter by reference to an aerial image [12].

Measuring the protection provided by a tree close to a canopy edge will obviously result in a higher proportion of the available solar radiation reaching an observer than if located near to a tree trunk. Similarly, measurements of solar ultraviolet protection made on the south side of a tree (Southern

Fig. 1. (a) A growing tree canopy that continually refreshes its leaf cover and grows in size can provide sustained solar ultraviolet protection for the life of the tree. *Araucaria bidwillii*, 19.0 m high and canopy diameter 14.1 m, is shown at its measurement location, 27.6014°S, 151.9408°E. (b) Experimental apparatus including tripod, video camera, neutral density filter and fish eye lens attachment are used to measure the effective sky view underneath *Araucaria bidwillii*.
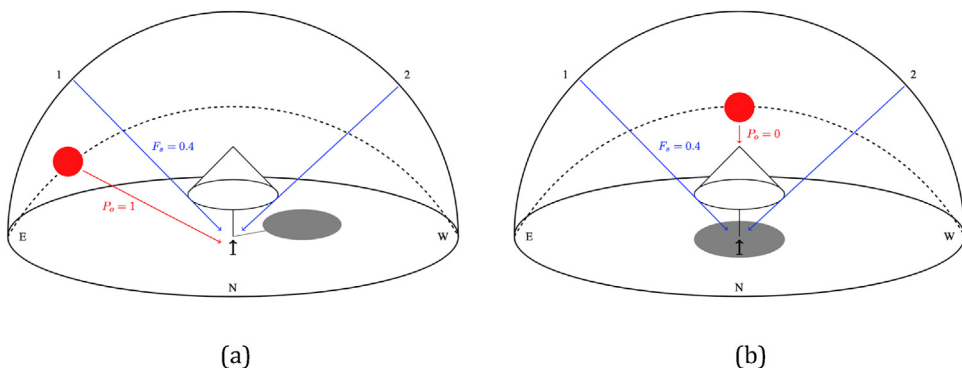

Fig. 2. (a) Tree canopy model showing the northern celestial traversal of the solar disc during the early morning (Southern Hemisphere). The solar disc (red circle) at this period is unobstructed by the tree canopy ($P_o = 1$) and reaches the observation point (marked by an arrow and north of the tree). The canopy shadow extends to the south-west and past the observation point. In this example case, 40% of the sky is visible ($Fs = 0.4$) from the observation point with diffuse solar radiation being blocked by the canopy between points 1 and 2. (b) Tree canopy model showing the northern celestial traversal of the solar disc at noon (Southern Hemisphere). In this case the solar disc is obstructed by the tree canopy ($P_o = 0$) which casts a shadow over the observation point. From this point, 40% of the sky is still visible ($Fs = 0.4$) and will contribute to the total solar radiation reaching the surface.

hemisphere) will block a greater proportion of the sky view than if made on the northern side. The chosen observation point therefore represents a conservative limit for determining protection standards for tree canopies. A point midway between the canopy edge and tree trunk also represents the position most likely to be visited by persons utilising tree shade and is a location that may be chosen fairly for any tree, independent of its size.

The sky fraction from the observation point is measured by video image analysis to take into account the typical movement of the canopy. Video capture was completed for our example using a 4k hi-resolution video camera (GoPro Hero5, USA) fitted with a fish eye lens and 25% transmission neutral density filter to minimise lens bloom (Celestron ND 96, USA). The camera was fixed to a tripod and levelled at 1 m above the ground surface (Fig. 1b). The selected camera height of 1 m represents the minimum canopy height above the ground at which a tree is likely to be included in a survey or shade
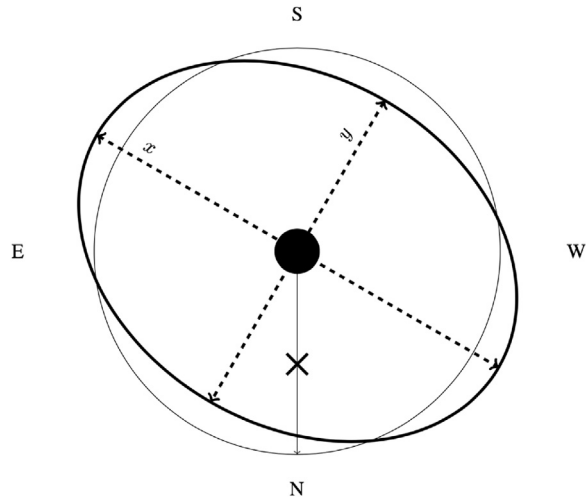
Fig. 3. Canopy observation point (marked by a cross) underneath an elliptical tree canopy (outlined in bold) is midway from the tree trunk (filled circle) to the approximate circular canopy circumference. Approximate canopy circumference has a radius equal to the average of *x* and *y* marked in the Figure.

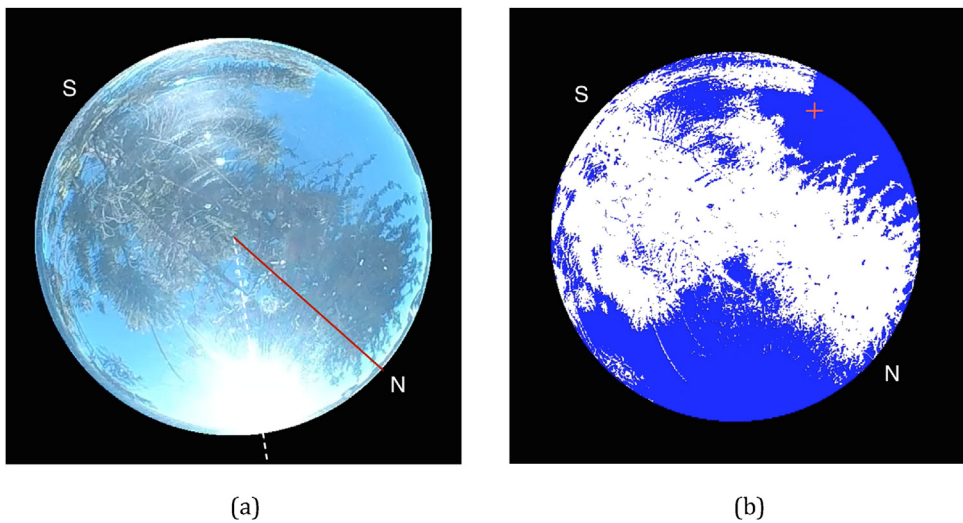(a)   (b)

Fig. 4. (a) Unprocessed canopy image of *Araucaria bidwillii* showing the white doted azimuth angle passing through the centre of the solar disc at local time of video recording (az = 320°). The red line indicates the fixed position of the meridian, 40° from the solar azimuth. (b) Processed canopy image of *Araucaria bidwillii* with surface objects and solar disc removed. The calculated position of the Sun at 8:00 am on 21 December 2018 is shown as an orange cross in the top right of the processed image (Po = 1 and Fs = 0.60).

audit, as trees with canopies extending to the ground would be difficult for pedestrians to access for public use. When the GoPro video camera image area is set to narrow and fitted with the fish-eye lens attachment, the Field of View (FOV) of the canopy camera extended to 140°, representing a respective solar zenith angle range (SZA) of 0 to 70°.

In our example, the sky fraction underneath the tree canopy was measured for a period of 180 s (1 frame per second) under cloud free conditions. This sample time is taken to represent the typical

movement of the tree canopy. Models that require assessment of shade in different environments may similarly be derived by video sampling over longer periods, during different seasons or during periods of high wind.

Video image processing was completed in MATLAB (R2014b, The Mathworks Inc). Classification of tree canopy and sky pixels from the recorded video frame data was based on the relative proportion of Blue and Red pixel image data following post processing to remove surface objects and the solar disc. Surface objects were removed by reducing the SZA range of the recorded canopy video to 65°. In the tree canopy model, the region of the sky hemisphere from SZA 65 to 90° that was not imaged was set to be free of obstruction. Thus, during early morning and late afternoon periods, direct solar radiation was assumed to reach the canopy observation point. This region of sky, closest to the horizon represents $\frac{5}{18}$ or 28% of each processed sky fraction.

In the processed video, the image of the solar disc was removed to prevent misidentification of potentially bright solar disc images as part of the tree canopy. This was achieved by locating pixels with saturated Red and Blue channels. To remove the solar disc from each video frame, pixels with saturated Red and Blue channels were changed to Blue sky pixels, (Blue = 255 and Red = 0). Fig. 4(a) shows a single canopy video frame recorded underneath *Araucaria bidwillii* and Fig. 4(b) shows the same frame post-image processing to remove surface objects and the solar disc. Hence, the sky fraction from the observation point is calculated according to:

$$F_s = \left(\frac{B}{T} \times \frac{13}{18} \right) + \frac{5}{18} \qquad (5)$$

Method application

Calculation of solar position

I_s(UV) was calculated during daylight hours (SZA < 90°) in five-minute intervals for the 2018 calendar year according to Eq. (1) by determining whether the direct solar UV component would
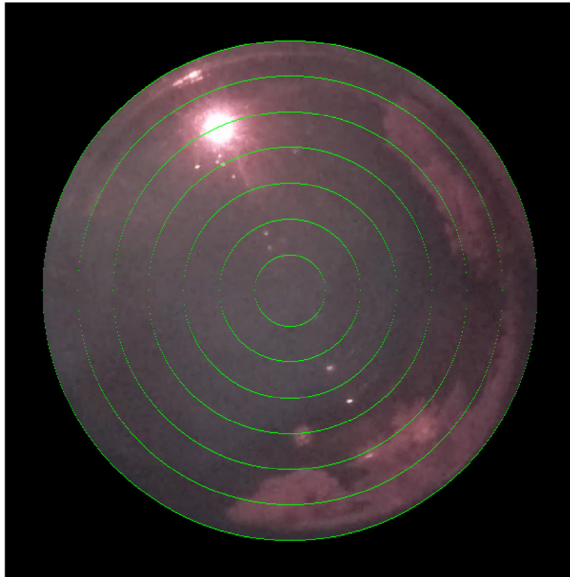

Fig. 5. Concentric circles of known pixel radius represent SZA limits which can be derived from a time lapse recording. A darker filter is used to reduce lens bloom under an unobstructed sky. The sun is shown at SZA 50.4o, 10:31 am 19 July 2018, 25.256°S, 152.823°E. Concentric circles represent SZA limits of 10°, 20°, 30°, 40°, 50°, 60° and 70°.

be obscured by the tree canopy at each of these times. The direct and diffuse solar UV irradiance components of I_s(UV) were determined for cloud free conditions at each five-minute interval of the year according to the surface UV irradiance algorithms of Green et al. [13], Green et al. [14], Schippnick & Green [15] and Rundel [16].

The modelled solar irradiance components evaluated for each five-minute interval of the year are used to derive the annual variation in SPI and UPF once the position of the sun is known with respect to the moving tree canopy (Eqs. (3) and (4)). Here, P_o was taken as 1 if the solar disc was located in the position of a processed Blue sky pixel of a respective video frame, and 0 if blocked by the tree canopy (white pixels in Fig. 4b). Video frames were cycled at each five-minute solar position interval. Therefore P_o could vary between 0 and 1, depending on the modelled position of the solar disc for the time of day and year, and the moving position of the processed canopy. The solar position per daylight five-minute interval of the year was calculated according to the algorithm of Michalsky [17] and fixed to each processed video frame in SZA and azimuth (video animations included in supplementary material).

SZA frame function

The position of the solar disc in a hemispherical view of the sky is linearly related to the zenith [18]. The position of the solar disc was determined in our example every five-minutes in an annual canopy frame iteration cycle by calculating the angular separation of the expected solar position for the time of day and year from the zenith. This was plotted onto each video frame as the changing radial position of the solar disc for the respective SZA.

The function describing the video frame pixel radius of the expected solar position was derived through comparison of concentric circles of known radius drawn onto time lapse video frames recorded in an unobstructed open sky environment (Fig. 5). For a tree canopy model, this can be used to derive a linear function for a fish eye lens attachment relating the lens image radius to the SZA. For the experimental apparatus utilised in this study,

$$R = 3.719\theta + 0.1. \tag{6}$$

Here, R is the rounded radius in pixels for placing the solar disc, extending from 0 at SZA 0° to 240 pixels at 65°. In the Equation, θ is the SZA in degrees. The solar azimuth for each five-minute annual time interval was used to fix the position of the solar disc relative to local North where 0° in azimuth is determined as the difference in decimal degrees from the solar disc azimuth angle recorded at the time the tree canopy video is taken (Fig. 4a).

Solar path and seasonality

Figs. 6 and 7 model the influence of *Araucaria bidwilli* during the seasonal extremes of the respective Southern hemisphere summer (21 December 2018) and winter solstice (21 June 2018). In Figs. 6a and 7a, the position of the sun is calculated and traced with respect to a static video frame to illustrate the influence of the tree canopy with time of day. Plots of the diurnal variation in SPI and UPF (Figs. 6b and 7b) are shown for the moving tree canopy, cycling every 180 frames. In both the summer and winter cases, at daybreak (and near sunset) the sun is well below the minimum SZA of 65° to be influenced by the processed tree canopy. Therefore, at times of day when the sun is outside the 65° processed canopy limit, the SPI and UPF remain low, being influenced only by the diffuse UV and available sky fraction, Fs at the observation point. In the given examples, when the position of the solar disc reaches the processed tree canopy, the SPI and UPF increase dramatically as the direct solar UV component is effectively blocked near noon by an overhead branch (Figs. 6a and 7a).

Seasonal variations in the length of day and solar celestial path, reaching near the zenith in summer and remaining closer to the horizon in winter also influence the modelled SPI and UPF. These variations can be modelled by taking site latitude into account. For both the summer and winter cases illustrated in Figs. 6 and 7, the SPI and UPF peak at solar noon (when the daily solar UV irradiance is greatest). In summer, the SPI and UPF reach their maximum annual values provided the noontime sun
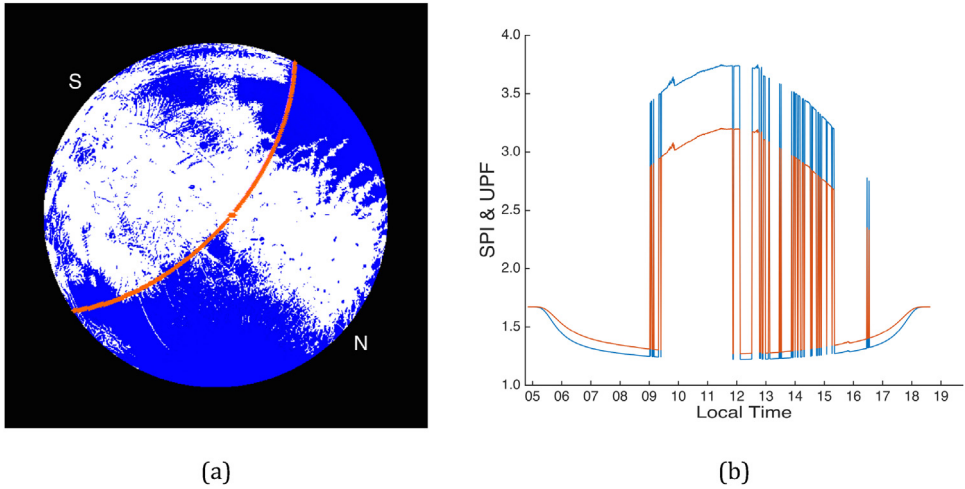
(a)   (b)

Fig. 6. Solar celestial path calculated for each minute of the day and relative to 1 of 180 processed video frames for *Araucaria bidwillii* on 21 December 2018, 6:55 am (SZA 65°, top right) to 4:35 pm SZA 65°, bottom left). (b) Calculated SPI (blue) and UPF (orange) of *Araucaria bidwillii* for each plotted solar position between 5:00 am and 7:00 pm, 21 December 2018.
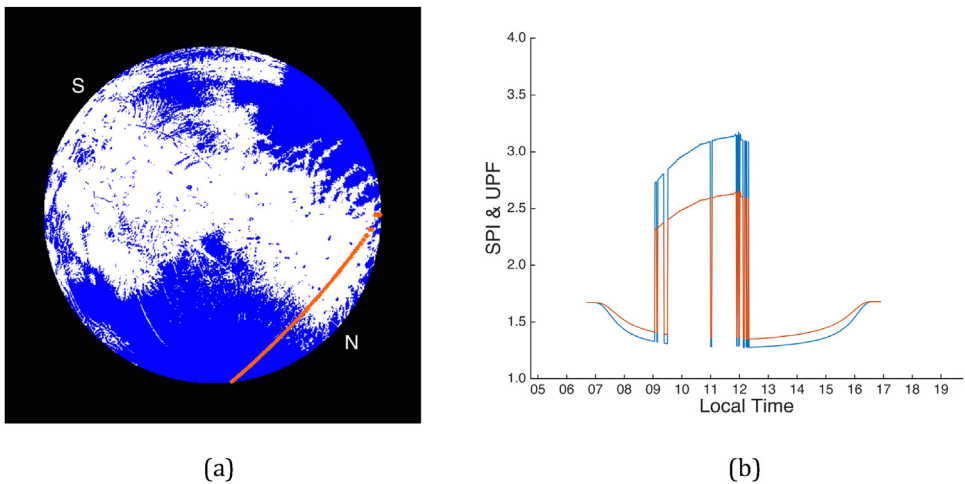

(a)   (b)

Fig. 7. Solar celestial path calculated each minute of the day and relative to 1 of 180 processed video frames for *Araucaria bidwillii* on 21 June 2018, 9:05 am (SZA 65°, middle right) to 2:30 pm (SZA 65°, bottom). (b) Calculated SPI (blue) and UPF (orange) of *Araucaria bidwillii* for each plotted solar position between at 5:00 am and 7:00 pm, 21 June 2018.

can be blocked by the tree canopy. However, as demonstrated by the rapid rise and fall of the modelled SPI and UPF between 12:00 and 15:00 local time (Fig. 6b), the effectiveness of a given tree canopy in reaching a maximum SPI (or UPF) at noon is also dependent on the position of canopy leaves and branches.

Fig. 8 presents the annual variation in SPI and UPF of *Araucaria bidwillii* calculated in five-minute intervals for the tree's Southern hemisphere site. As shown for the study tree, the maximum SPI (or UPF) occurs at and near the summer solstice, when the greatest annual direct solar UV irradiance is obscured by the protecting canopy. Peak protection factors drop to their minimum annual value at and near the winter solstice. A tree canopy in which the majority of leaves and branches are displaced from

the central trunk (or zenith) may not necessarily reach its annual peak UV protection at the summer solstice. Thus, the protection provided by each tree canopy is effectively unique and dependent upon the structure of the tree. By taking an annual average of both the SPI and UPF, the quality of protection provided by a tree can however be quantitatively assessed and compared between different species and tree specimens.

Method validation

Standardised assessments of the solar UV protection provided by a tree canopy are derived here in terms of the SPI and UPF by application of the surface approximations of Grant et al. [2] (Eq. (1)) for a set observation point, located midway between the tree canopy extremity and tree trunk on its northern side. As shown, the protection provided by a tree canopy will vary with time of day and season, depending upon the position of the solar disc.

To take into account the natural movement of the tree canopy, video image analysis was conducted to simulate the likely canopy movement under realistic conditions. Using this technique, the SPI and UPF can approximate the variation in ultraviolet exposure at the observation point for any time of day or year and at any site latitude. To demonstrate this, the erythematic UV irradiance was derived underneath *Araucaria bidwillii* (27.601 °S, 151.941 °E) using the modelled UPF of the tree canopy between 6:10 am and 5:10 pm on 7 November 2018. The erythematic UV irradiance was derived by rearrangement of Eq. (4), where:

$$\int_{290}^{400} I_S(\lambda) A_{ery}(\lambda) = \frac{\int_{290}^{400} I_{dir}(\lambda) A_{ery}(\lambda) d\lambda + \int_{290}^{400} I_{diff}(\lambda) A_{ery}(\lambda) d\lambda}{UPF} . \tag{7}$$

In deriving the erythematic UV irradiance, the erythemally effective ambient,

$$I(UV) = \int_{290}^{400} I_{dir}(\lambda) A_{ery}(\lambda) d\lambda + \int_{290}^{400} I_{diff}(\lambda) A_{ery}(\lambda)$$

was simultaneously measured in five-minute intervals between 6:10 am and 5:10 pm on 7 November by a 501 UV biometer (Solar Light Co, PA, USA). This meter is located within proximity of *Araucaria bidwillii* and is permanently mounted less than 1 000 m from the tree site at the University of Southern Queensland (27.603 °S, 151.930 °E).

Because the UPF defines the relative protection of a tree canopy relative to the available ambient, the surface UV underneath the tree can be estimated, irrespective of the ambient UV at the time. A model can therefore be derived that takes into account the cloud condition, provided ambient irradiance measurements are available at or in proximity to a given tree site. Fig. 9 compares the measured ambient erythematic UV irradiance to the modelled UV derived from the canopy UPF of *Araucaria bidwillii* on 7 November 2018. On this day, cloud cover influenced the measured ambient UV irradiance. This is most noticeable as dips in the diurnal UV irradiance after approximately 11:00 am local time (Fig. 9a).
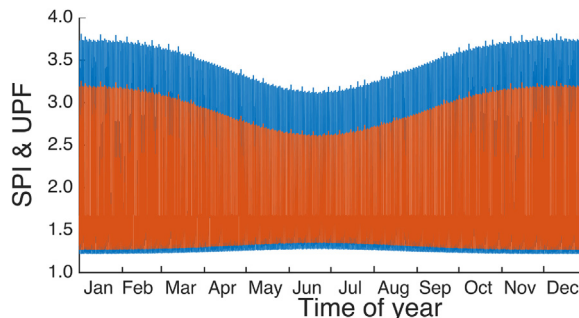

Fig. 8. Annual variation in SPI (blue) and UPF (orange) of *Araucaria bidwillii* at a Southern hemisphere site.
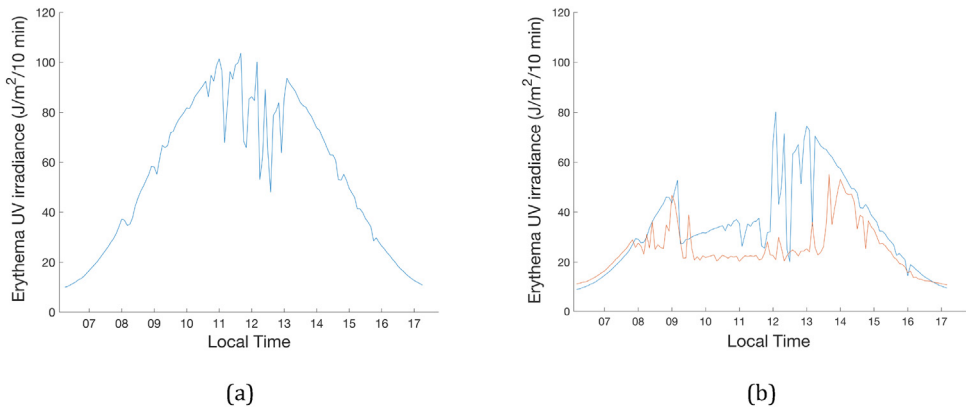
Fig. 9. Ambient erythema UV irradiance recorded in proximity to *Araucaria bidwillii*, 7 November 2018. (b) Measured (orange) north side observation point surface UV irradiance underneath *Araucaria bidwillii*, 7 November 2018 compared against the expected UV irradiance derived from the dynamic canopy UPF (blue). The dynamic canopy UPF is derived from video assessment taken 15 July 2018 at the same observation point.

For the duration of the modelled exposure period, I_S(UV) was also measured in five-minute intervals underneath the tree canopy using a portable PMA2100 radiometer with fitted erythematic sensor (model PMA2102 SUV, Solar Light Co. PA, USA) placed at the north side observation point of *Araucaria bidwillii*, 1 m above the ground surface. The field PMA2100 radiometer was calibrated to the 501 ambient UV Biometer with output recorded in J/m^2/10 min. The measured erythematic UV irradiance underneath *Araucaria bidwillii* is compared to the expected irradiance derived from the canopy UPF in Fig. 9b.

The comparison between the measured and expected UV surface irradiance underneath *Araucaria bidwillii* shows clearly the influence of the north facing tree branches from approximately 9:15 am to 1:30 pm. During this period, the erythema exposure falls sharply but continues to fluctuate as the solar disc passes between breaks in the tree canopy. The measured erythema UV irradiance falls below the expected UV irradiance from approximately 2:00 pm (35.1 °SZA). At this time, and in the period 7:00 am to 4:15 pm the sun is within the 65 °SZA limit of the canopy model. Thus, surface obstructions and objects located in vicinity of the local horizon which reduce the sky fraction under the tree canopy and physically influence the measured UV irradiance, often differ with the expected predictions which are limited to a 130 °FOV and assume a clear horizon. As a result, local UV irradiance predictions under the modelled dynamic tree canopy are generally higher than the measured irradiance.

For a pedestrian, moving either side of the observation point can also change the received personal irradiance under a living tree canopy, particularly if canopy branches are close to the observation point where slight movement from this point can have a potentially significant influence on personal shade patterns. Here, measurements taken underneath *Araucaria bidwillii* and plotted for 7 November 2018, were taken several months after the tree canopy video analysis was recorded (under cloud free conditions) on 15 July 2018. Changes in canopy structure, growth, regrowth or damage (and pruning) can all influence the received UV irradiance under a living tree canopy.

Conclusion

A method for standardising and making comparative assessments of the solar UV protection provided by a living tree canopy has been developed utilising video image analysis and solar path tracking for application across a range of site latitudes. The technique is given the term, intelligent shade audit, taking into account the importance of standardisation in measurement and given the technique can model minor variations in a dynamic tree canopy for any time of day (or year) and at any required tree site.

The developed technique includes for the first time an assessment of the ultraviolet protection underneath a moving (dynamic) tree canopy showing how clear fluctuations in the SPI and UPF can be determined over relatively short, daily time scales. This included testing against a field radiometer, demonstrating the use of site-specific dynamic canopy modelling in forecasting the real-time UPF under a moving tree canopy. A method for calculating longer term seasonal and annual shade characteristics of a living tree canopy has also been presented. This new methodology, employing video image analysis will provide an accessible technique to planners and designers interested in optimizing ultraviolet protection by tree shade. This method has been developed therefore to aide government, planning, design, built environment and health authorities to better plan for the provision of tree shade in public spaces, but also to enable standardised canopy assessment in situ.

Acknowledgements

Appendix A. Supplementary data

Supplementary material related to this article can be found, in the online version, at doi:https://doi.org/10.1016/j.mex.2019.07.013.

References

[1] N.J. Downs, L. Baldwin, A.V. Parisi, H.J. Butler, J. Vanos, M. Beckman, S. Harrison, Comparing the annualized dynamic shade characteristics of twenty-one tree canopies across twenty-six municipalities in a high ambient UV climate, Queensland – Australia, Appl. Geogr. 108 (2019) 74–82.
[2] R. Grant, G. Heisler, W. Gao, Esimation of pedestrian level UV exposure under trees, Photochem. Photobiol. 75 (2002) 369–376.
[3] B. Diffey, Ultraviolet radiation and human health, Clin. Dermatol. 16 (1998) 83–89.
[4] R. Gallagher, T. Lee, Adverse effects of ultraviolet radiation: a brief review, Prog. Biophys. Mol. Biol. 92 (2006) 119–131.
[5] Commission Internationale de l'Eclairage (CIE), Erythema Reference Action Spectrum and Standard Erythema Dose ISO 17166:1999 (CIE S 007/E:1998), (1998) .
[6] N. Agar, G. Halliday, R. Barneton, H. Ananthaswamy, M. Wheeler, A. Jones, The basal layer in human squamous tumors harbors more UVA than UVB fingerprint mutations: a role for UVA in human skin carcinogenesis, Proc. Natl. Acad. Sci. U. S. A. 101 (2004) 4954–4959.
[7] M. Grigalavicius, J. Moan, A. Dahlback, A. Juzeniene, Daily, seasonal and latitudinal in solar ultraviolet A and B radiation in relation to vitamin D and risk for skin cancer, Int. J. Dermatol. 55 (2015) e23–e28.
[8] K. Hoffmann, K. Kaspar, P. Altmeyer, T. Gambichler, UV transmission measurements of small skin specimens with special quartz curvettes, Dermatology 201 (2000) 307–311.
[9] W. Bruls, J. Van Der Leun, Forward scattering properties of human epidermal layers, Photochem. Photobiol. 40 (1984) 231–242.
[10] H. Gies, C. Roy, G. Elliott, W. Zongli, Ultraviolet radiation protection factors for clothing, Health Phys. 67 (1994) 131–139.
[11] B. Diffey, Human exposure to ultraviolet radiation, J. Cosmet. Dermatol. 1 (2003) 124–130.
[12] Google Maps, 2018. URL: https://www.google.com/maps/.
[13] A. Green, T. Sawada, E. Shettle, The middle ultraviolet reaching the ground, Photochem. Photobiol. 19 (1974) 251–259.
[14] A. Green, K. Cross, L. Smith, Improve analytic characterization of ultraviolet skylight, Photochem. Photobiol. 31 (1980) 59–65.
[15] P.F. Schippnick, A.E.S. Green, Analytical characterization of spectral actinic flux and spectral irradiance in the middle ultraviolet, Photochem. Photobiol. 35 (1982) 89–101.
[16] R. Rundel, Stratospheric Ozone Reduction, Solar Ultraviolet Radiation and Plant Life, Springer-Verlag, Berlin, 1986 chapter in Computation of Spectral Distribution and Intensity of Solar UVB Radiation.
[17] J. Michalsky, The Astronomical Almanac's algorithm for approximate solar position (1950-2050), Sol. Energy 40 (1988) 227–235.
[18] W. Gao, R. Grant, G. Heisler, J. Slusser, A geometric UV-B radiation transfer model applied to vegetation canopies, Argron. J. 94 (2002) 475–482.